Investigations and experiments of a new multi-layer complex liquid-cooled mirror

Yuling Lu (陆宇灵), Zuhai Cheng (程祖海),
Yaoning Zhang (张耀宁), Feng Sun (孙 锋), and Wenfeng Yu (余文峰)

State Key Laboratory of Laser Technology, Huazhong University of Science and Technology, Wuhan 430074

Received February 2, 2004

This paper describes a new multi-layer complex liquid-cooled Si mirror with 3 cooling ducts in Archimedes spirals. Utilizing the ANSYS program, the structure of the mirror is optimized and the thermal deformation model of the mirror is simulated. The simulation results show that the mirror has the following advantages: very small amount of surface deformation, uniform distribution of temperature and surface deformation, and fast surface shape restoration. The results of the experiments of thermal deformation and the surface restoration are accurately mapped to the simulation results.

OCIS codes: 140.3410, 140.3460.

Liquid cooling has always been an effective method to minimize the deformation of resonators' mirrors in high-power laser devices. By designing the appropriate structure and utilizing fluid-filled cooling ducts to absorb the heat, mirrors can be cooled and the deformation of the mirrors can be limited. The heat exchange between the fluid and the mirrors' body depends on the properties of the fluid and the substrate of the mirrors, the flow state of the fluid, and the structure of the flow channels (cooling ducts). Generally the flow states are defined into laminar flow, transition flow, and turbulent flow, with turbulent flow representing the highest heat transfer coefficient. The structure of the cooling ducts influences the efficiency of the heat exchange, thus better designs mean better efficiency. Cheng *et al.* conducted extensive experiments on multi-layer Cu mirrors[1].

When a laser beam interacts with a liquid cooled mirror, the energy of the laser beam is transferred to the mirror's body and then into the fluid. As a result, the properties of the mirror's substrate are factors influencing the heat exchange. In Ref. [2], the thermal conductivity, the coefficient of thermal expansion, the stress parameters, and the manufacturing process of silicon, tungsten, molybdenum, copper, carborundum, beryllium, aluminum, and nickel are compared. Silicon was chosen as an appropriate material for the mirror's substrate in a high power laser device, due to the ease of the manufacturing process, and its low coefficient of thermal expansion and high thermal conductivity.

The design of the new water-cooled mirror specifies structure of the cooling ducts and size, the inlet and outlet of the water fluid, the flow paths of the fluid, and the control of the water pressure and flow rate.

The multi-layer complex liquid-cooled Si mirror which we designed is shown in Fig. 1. In Fig. 1(b), it consists of 3 Si layers. The illumination layer is a circular Si plate with a thickness of 2.3 mm and a diameter of 80 mm. On the back of the illumination layer is the tightly coupled Si substrate (the ducts layer) with the same diameter and a thickness of 10 mm. Three 10-mm deep Archimedes-spiral channels are etched in the ducts layer (that is, the height of the ducts is equal to the thickness of this layer, acting as cooling ducts). The ducts have the same length and interleave at 2 mm. Their inlets are very close to the center of the ducts layer and are evenly spaced in the shape of an equilateral triangle, in order to alleviate the entry impact. The outlets are very close to the fringe of the ducts layer, and are also evenly spaced in the shape of an equilateral triangle. The last layer, the airproof layer, covers the ducts layer to seal the ducts, and the 3 layers are welded together by the vacuum welding technology with aluminum as solder. A parent inlet leads the flow equally into the 3 inlets. The Archimedes spirals, which direct the ducts interfluent, help to distribute the heat and pressure evenly.

In order to reduce the thermal resistance, a thin illumination layer is preferred. However, an overly thin illumination layer loses rigidity, which in turn increases deformation, especially deformation caused by the pressure surge of water fluid. Thus there exists a need for

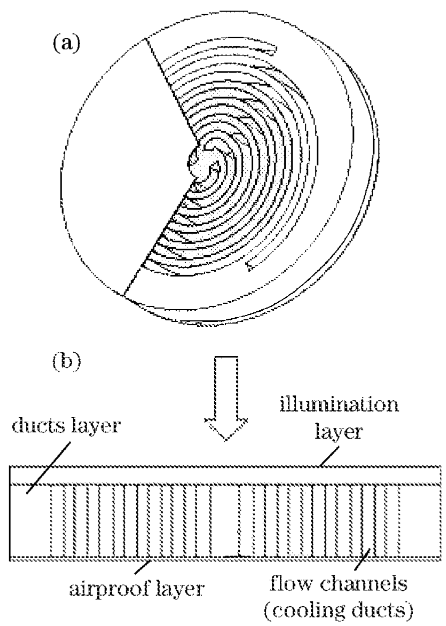

Fig. 1. The shape (a) and the axial cutaway diagram (b) of the multi-layer complex liquid-cooled Si mirror.

the proper thickness of the illumination layer, and the proper design of the mirror.

A simulation model of the mirror, shown in Fig. 1, is established with the well-known finite-element-method program – ANSYS (published from ANSYS Inc., United States). In this model, the following conditions are assumed: the coolant water temperature at the inlets is 20 °C, the velocity of flow is 1.6 m/s, coefficient of convective heat transfer is 9000 W/m^2K, water pressure is 1.5×10^5 Pa, a circular laser facula is on the mirror surface and the net absorption of the mirror surface is 100 W, the heat convection between mirror body and ambient air does not exist, and the constraint shift of the mirror's fringe is zero.

The optimal size differs according to different flow velocities and pressures. The premise of the design, with the flow rate of 80 ml/s and fluid pressure of 1.5×10^5 Pa, calls for an optimized structure of the mirror with the duct's depth of 10.2 mm, breadth of 2.5 mm, and the length of a duct of 240.3 mm. Based on this structure, the simulating calculation results are: the highest temperature is 25.74 °C, the lowest temperature is 20.09 °C, and the axial deformation is 0.174 μm. The hydrostatic pressure is also considered in the calculation. The cooling effect has proven to be significant. As shown in Fig. 2, at time of laser irradiation of 5 s, the curves representing the thermal distribution and the deformation of the mirror's surface flatten near the mirror's surface center. The peak value of the distortion of the shape of the facula area is approximately 0.0825 μm, and the peak value of the deformation on mirror's surface is approximately 0.174 μm. The maximum temperature and the maximum surface deformation varying with respect to time are shown in Fig. 3. Compared with a solid Si

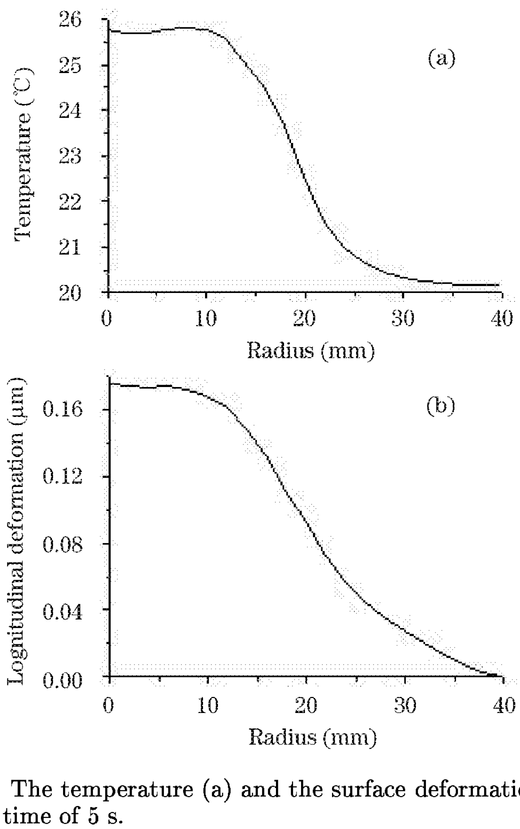

Fig. 2. The temperature (a) and the surface deformation (b) at the time of 5 s.

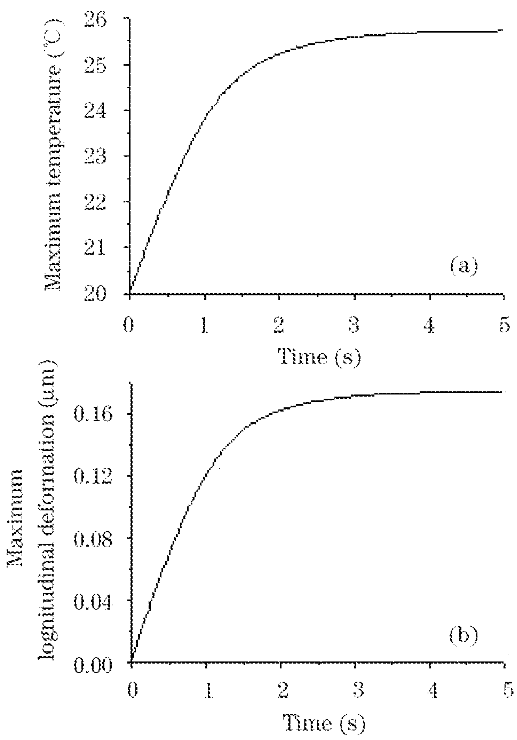

Fig. 3. The maximum temperature (a) and the maximum surface deformation (b) varying with respect to time.

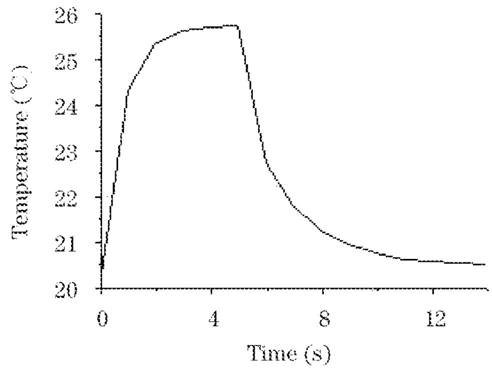

Fig. 4. The cooling curve of the multi-layer complex liquid-cooled Si mirror.

mirror, the multi-layer complex liquid-cooled Si mirror reaches plateau in a much shorter time. The maximum temperature stabilizes at approximately 24.8 °C in 3 s, and the maximum deformation at approximately 0.174 μm in 2.3 s. In contrast, it is impossible for a solid Si mirror to reach plateau in 5 s.

Because of the high coefficient of convective heat transfer, the multi-layer complex liquid-cooled Si mirror is cooled fast as shown in Fig. 4.

The measurements of the hydraulic pressure, thermal deformation, and cooling effect on this mirror are conducted with the measurement system shown in Fig. 5.

The system operates by the following method: the laser beam emitted from He-Ne laser travels through reflecting mirror, is focused on an aperture which is on the focal plane of the collimation object lens (the autocollimator), finally is collimated into plane wave, and subsequently split into two beams by the beam splitter.

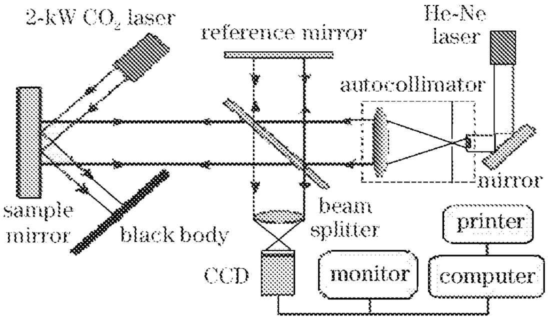

Fig. 5. The principle of the measurement system.

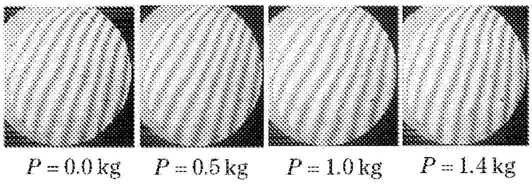

Fig. 6. The mirror surface interference patterns under different hydrostatic pressures (P) of the coolant water.

Table 1. The Peak Deformations on Surface (D) Corresponding to Different Hydrostatic Pressures (P)

P (kg)	0.5	1.0	1.4
D (μm)	0.017	−0.026	0.024

One of the beams will be reflected onto the reference mirror and go back to the original location, and is named the reference beam; the other beam will go through the beam splitter and travel towards a sample mirror, then will be reflected by the sample mirror's surface, and interfere with the reference beam. The interference pattern is turned into images by photograph lens, then intercepted by CCD and transformed into electrical signals. The image-capturing card will capture the electrical signals and send them to the computer for processing. Curvature radius and surface model of the sample mirror are measured this way.

In this experiment, water is utilized as the cooling fluid. Through hydrostatic pressure and the flow rate manipulation by valve adjustment, the interference patterns and the peak deformation values of the multi-layer complex liquid-cooled Si mirror are experimentally obtained.

From Fig. 6 and Table 1, we can conclude that under normal air pressure, the multi-layer complex liquid-cooled Si mirror is not sensitive to the hydrostatic pressure of the coolant water.

In addition, as soon as the valve is adjusted, the interference patterns fluctuate and only stabilize after 2.5 s due to the sudden variation of the flow rate and the pressure. In order to have a consistent baseline, the water pressure must stabilize before laser output.

After the hydrostatic pressure of the coolant water stabilizes, the interference patterns appear micro-pulse at higher frequency and smaller amplitude due to the micro-pulse of the fluid pressure and the velocity acting on

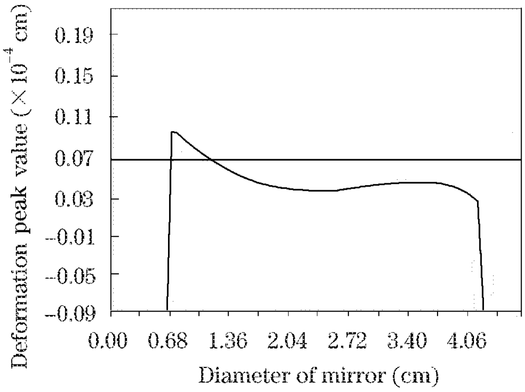

Fig. 7. The mirror surface pulse when hydrostatic pressure is 1 kg.

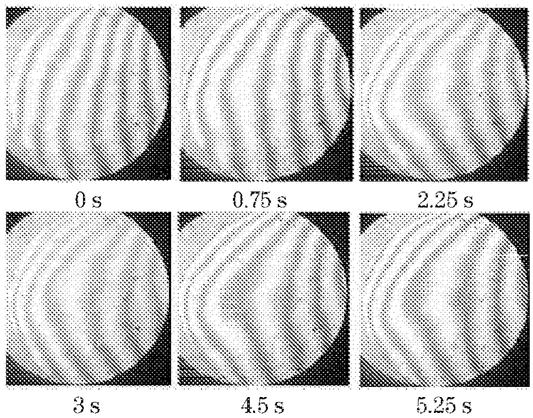

Fig. 8. The mirror surface interference patterns at different moments.

ducts' inner wall. The phenomenon shown in Fig. 7 is termed mirror surface pulse, which oscillates at the frequency of 2000 Hz[3−5]. Michael defined the pulse pressure caused by flow velocity pressuring flow channel as

$$F'(t) = \iint_A p'(x,t)\cos\theta(x)\mathrm{d}A, \tag{1}$$

where $p'(x,t)$ stands for the pressure on the ducts' inner wall, and $\theta(x)$ stands for the angle of circumference of the inner ducts. Consequently the power spectrum density (PSD) function of $F'(t)$ is given by

$$\mathrm{PSD}_{F'} = \frac{Q^3\beta^2 LK}{NA}, \tag{2}$$

where Q stands for volume flow rate, β for density, L for length of the duct, K for the flow separation constant, N for the number of the branches, and A for the cross-section area of the duct. According to Eqs. (1) and (2), utilizing fluids of lower density, reducing the length of the ducts, and enlarging the area of the inlets can all decrease the surface pulse.

The mirror surface interference patterns at different moments are shown in Fig. 8. Measurements are made when the flow rate is 80 ml/s, hydrostatic pressure is 1.25×10^5 Pa, and the net absorption of the mirror surface is 100 W. At the same time, the peak value of the surface deformation varying with respect to time is shown in Fig. 9, compared with the results of numerical calculation. The experiment shows that the surface deformation increases rapidly and reaches 0.117 μm at 0.75 s. Afterwards the increase rate declines, the peak value of the surface deformation reaches 0.187 μm at 3 s. The temperature and the deformation value stabilize subsequently, and the peak value of the surface deformation reaches 0.186 μm at 5.25 s.

As shown in Fig. 9, the results of experiments and calculation are almost the same, but the experimental results are slightly higher. There exist two main reasons: 1) the distribution of the facula in calculation is assumed to be uniform, but in experimentation it is not, thus the uneven distribution causes localized temperature rises and increases the surface deformation; 2) the quality of vacuum welding connecting the illumination layer and the ducts layer is imperfect, so that the heat transfer from the illumination layer to the ducts layer is slightly impeded.

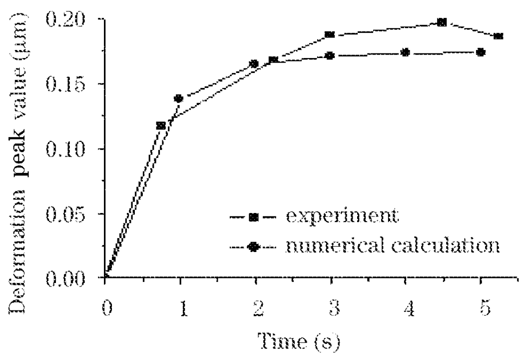

Fig. 9. The peak value of the surface deformation varying with respect to time.

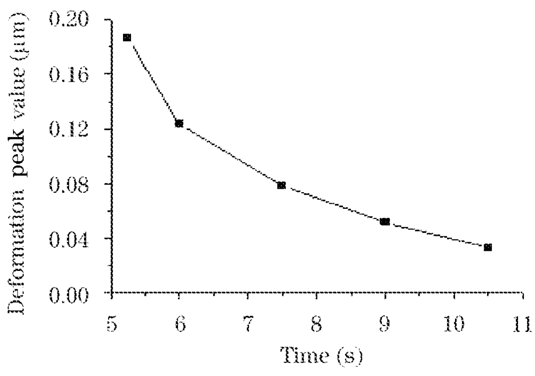

Fig. 10. The cooling process of the multi-layer complex liquid-cooled Si mirror.

The laser illumination is shut down at 5.25 s, but the fluid still flows at the flow rate of 80 ml/s. The measurement system records the subsequent variation of the mirror surface, and the peak value of the surface deformation is shown in Fig. 10. After stopping laser illumination, the surface deformation decreases 0.063 μm in 0.75 s, the peak value of the surface deformation drops down to 0.038 μm at 10.5 s. The experiment demonstrates that the mirror's surface restores fast enough to be used repeatedly in extremely short time intervals. This observation possesses great significance in high power laser devices. In the experiment, the fluid temperature is 23 °C and the air temperature is 26 °C while both are assumed to be 20 °C in the numerical calculations shown in Fig. 4, therefore the cooling process in the experiment is faster than that in calculation.

A new multi-layer complex liquid-cooled Si mirror with three cooling ducts in Archimedes spirals is presented in this paper. The mirror has the advantages of minimal surface deformation, uniform distribution of temperature and surface deformation, and fast surface shape restoration.

By utilizing ANSYS program, the structure of the mirror is optimized when the flow velocity is assumed to be 1.61 m/s and the hydrostatic pressure to be 1.5×10^5 Pa, and thermal deformation model of the mirror is established to simulate the thermal deformation process. The simulation results illustrate that the temperature and deformation on surface significantly decrease, and the mirror can stabilize in 3 s. It is also shown in this simulation that after stopping laser illumination, the temperature on mirror's surface declines to 20.7 °C in 5 s (both the temperature of the mirror and the fluid are assumed to be 20 °C), fast enough to meet the demands of practical applications.

Experimental results are very similar to simulation results. The experimental results also prove that, under normal air pressure, the multi-layer complex liquid-cooled Si mirror is not sensitive to the hydrostatic pressure of the coolant water.

Y. Lu's e-mail address is redsnowland@hotmail.com.

References

1. Z. H. Cheng, Y. N. Zhang, Z. M. Du, G. Ku, and F. Li, High Power Laser and Particle Beams (in Chinese) **9**, 418 (1997).
2. H. A. Bender, W. T. Silfvast, K. M. Beck, and R. K. Singh, Appl. Opt. **32**, 6999 (1993).
3. J. Arthur, Opt. Eng. **34**, 441 (1995).
4. G. Marot, Opt. Eng. **34**, 426 (1995).
5. M. J. Laughlin, Opt. Eng. **34**, 321 (1995).